Submitted to the Journal of Atmospheric Sciences — special issue on "Jets", June 2006

The direct stratosphere–troposphere interaction

MAARTEN H. P. AMBAUM[1]

Department of Meteorology, University of Reading, Reading, United Kingdom

[1]Corresponding author address: Dr. Maarten Ambaum, Department of Meteorology, University of Reading, P.O. Box 243, Reading, RG6 6BB, United Kingdom. Email: m.h.p.ambaum@reading.ac.uk

ABSTRACT

Potential vorticity anomalies in the stratosphere have a direct effect on the circulation in the troposphere through geostrophic and hydrostatic equilibrium. The potential vorticity viewpoint clarifies the interpretation of typical model experiments of stratosphere–troposphere interaction. The importance of planetary rotation to the strength of the interaction is singled out by performing inversion experiments on an idealized stratospheric vortex in gradient wind balance at varying planetary rotation rates. It is argued that the full balanced structure of the atmosphere has to be taken into account when considering coupling between the stratosphere and the troposphere.

1. The direct stratosphere–troposphere interaction

In a rotating stratified atmosphere, circulation changes are always associated with potential vorticity anomalies. Kleinschmidt (1954) calls these anomalies cyclonic “bodies” and he argues how these cyclonic bodies induce circulation changes, a property which has become known as invertibility in the later literature (Hoskins et al., 1985). Potential vorticity is materially conserved in an adiabatic atmosphere while in the presence of diabatic effects a flux form conservation law for potential vorticity can be formulated (Haynes and McIntyre, 1987). Because such a conservation law exists we can usefully put the locus of any circulation change at the inducing potential vorticity anomaly —its cyclonic body. This paper is concerned with tropospheric circulation changes for which the locus is in the stratosphere. I call this the direct stratosphere–troposphere interaction. Ambaum and Hoskins (2002, hereafter AH2002) found this direct effect to be substantial, explaining the main part of the amplitude of the observed stratosphere–troposphere interaction. Model results by Hartley et al.(1998) and Black (2002) similarly indicated a strong influence of stratospheric potential vorticity anomalies.

The potential vorticity viewpoint apparently contrasts with the more informal view that a light stratosphere does not have enough kinetic energy content to modify a heavy troposphere beneath; the pressure changes induced by shifting stratospheric circulations are modest when they are supposed to accelerate and decelerate a much heavier troposphere. The contrast becomes particularly salient if one considers the anelastic form of the quasi-geostrophic potential vorticity where background density is an explicit variable and the usual mid-latitude scalings are used. In this form the quasi-geostrophic potential vorticity q is:

$$\begin{aligned} q &= \beta y + \nabla^2\psi + \frac{f^2}{\rho_0}\frac{\partial}{\partial z}\left(\frac{\rho_0}{N^2}\frac{\partial\psi}{\partial z}\right) \\ &= \beta y + \nabla^2\psi - \frac{f^2}{HN^2}\frac{\partial\psi}{\partial z} + \frac{f^2}{N^2}\frac{\partial^2\psi}{\partial z^2}, \end{aligned}$$

with the usual notation for all symbols and with ρ_0 the background density profile which is assumed to decay exponentially with density scale height H. This density scale height does not vary much over the troposphere and stratosphere (perhaps 6–8km at mid to high latitudes). In the second form of the equation it becomes clear that density does not feature explicitly in the potential vorticity: a potential vorticity anomaly induces the same circulation anomalies irrespective of whether the anomaly is located in the light stratosphere or the heavy troposphere; there is vertical symmetry.

In this argument it is assumed that the stratosphere can support equally big potential vorticity anomalies as the troposphere. The relative vorticity anomaly and the stratification anomaly in the equations above are usually of similar magnitude; their ratio is called the Burger number and for most geometrically unconstrained flows the Burger number is close to one. As the stratosphere has plenty of circulation, it can certainly support large potential vorticity anomalies.[2]

The lower boundary brings in a vertical asymmetry in the argument outlined above. However, far enough from the boundary the symmetry is only slightly broken. The symmetry only refers to where the potential vorticity anomaly is introduced in the atmosphere. Because of the stratification there is an asymmetry in the upward and downward influence of any potential vorticity anomaly wherever it is placed. A more complete discussion can be found in AH2002 and Scott and Dritschel (2005a; 2005b) and we will refer to this difference in Section 3 below.

The potential vorticity viewpoint as advocated in AH2002 appears to depend heavily on the assumed geostrophic balance. Would in the absence of geostrophic balance the "light-stratosphere" argument become more applicable? In this paper we will relax the assumption of geostrophic balance by spinning down the planet and then see how the direct stratosphere–troposphere is affected. The theory and experimental set-up are described in the next Section. The results are discussed in Section 3, followed by a discussion and conclusion.

[2] The fact that Ertel potential vorticity is large in the stratosphere is not relevant here. The quasigeostrophic potential vorticity q is not trivially related to Ertel potential vorticity P; this is discussed in some detail in Charney and Stern (1962) and Hoskins et al. (1985). In fact, q is more similar to $\delta P/P$, which means that the fractional anomaly of Ertel potential vorticity rather than its absolute value is the dynamically active variable.

2. A vortex in gradient wind balance

If we approximate the stratospheric vortex as cylindrically symmetric and steady it is in gradient wind balance irrespective of the rotation rate of the atmosphere. Thus we can explore how the two viewpoints are connected by changing the rotation rate of the atmosphere. For simplicity we will consider a three layer atmosphere. The lowest layer is a notional troposphere, and the middle layer is a notional stratosphere, perhaps the lower to middle stratosphere. We then prescribe a particular vorticity distribution in the stratosphere and ask what the direct effect to the troposphere is. For low Rossby numbers we expect to reproduce the AH2002 results. We will further assume that the vortex lives on a polar f-plane. Layers are numbered starting from 1 for the troposphere —see schematic in Fig. 1.

In an N-layer system, hydrostatic balance in each layer relates the geopotential anomaly ϕ_i in layer i to the interface height perturbations h_i between layers i and $i+1$. This relationship can be succinctly written as:

$$\phi_i = (1 - n_i)\, gh_i + n_i\, \phi_{i+1}, \tag{1}$$

with $n_i = \rho_{i+1}/\rho_i$, and $n_N = 0$. All fields are assumed to be radially symmetric with radial coordinate r. The azimuthal velocity V_i is then in gradient wind balance with the geopotential:

$$\frac{\partial \phi_i}{\partial r} = \frac{V_i^2}{r} + fV_i \tag{2}$$

Each layer has a radially symmetric shallow water potential vorticity field P_i:

$$P_i = \frac{f + \xi_i}{D_i + h_i - h_{i-1}}, \tag{3}$$

with $h_0 = 0$ and the relative vorticity field ξ_i defined as:

$$\xi_i = \frac{V_i}{r} + \frac{\partial V_i}{\partial r}. \tag{4}$$

Note that the radial coordinate r increases in the opposite direction of the normal direction in a natural coordinate system.

Next we prescribe a vortex in layer 2 of our 3-layer system by prescribing the velocity/vorticity field in layer 2. The implied changes in geopotential and potential vorticity fields follow from the imposed balance conditions which will be dependent on the planetary vorticity f. By imposing a vorticity distribution in layer 2 the potential vorticity in layers 1 and 3 does not change, so we have:

$$\frac{f}{D_j} = \frac{f + \xi_j}{D_j + h_j - h_{j-1}}, \tag{5}$$

for both $j = 1$ and $j = 3$. We can now use Eq. 1 to rewrite the interface height differences as differences in geopotential to find:

$$\xi_1 = \frac{f\left(\phi_1 - n_1\,\phi_2\right)}{\left(1 - n_1\right)gD_1}, \text{ and } \xi_3 = \frac{f\left(\phi_3 - \phi_2\right)}{\left(1 - n_2\right)gD_3}. \tag{6}$$

Taking the radial derivative of these equations and substituting Eq. 2 and Eq. 4 leads to the final result:

$$\frac{\partial}{\partial r}\left(\frac{V_1}{r} + \frac{\partial V_1}{\partial r}\right) = \frac{f}{\left(1 - n_1\right)gD_1}\left(\frac{V_1^2}{r} + fV_1 - n_1\left(\frac{V_2^2}{r} + fV_2\right)\right), \tag{7}$$

and:

$$\frac{\partial}{\partial r}\left(\frac{V_3}{r} + \frac{\partial V_3}{\partial r}\right) = \frac{f}{\left(1 - n_2\right)gD_3}\left(\frac{V_3^2}{r} + fV_3 - \left(\frac{V_2^2}{r} + fV_2\right)\right). \tag{8}$$

These are both nonlinear second order equations for V_1 and V_3 respectively with a source term given as a function of V_2. The boundary conditions are $\lim_{r\to\infty} V_j = 0$ and $\lim_{r\to 0} V_j = 0$. After finding the velocity field in each layer, Eq. 2 can be integrated to reconstruct the geopotential in each layer setting the integration constant by $\lim_{r\to\infty} \phi_i = 0$. Equation 1 can then be used to reconstruct the interface heights. The geopotential anomaly can be related to a pressure anomaly by scaling with ρ_i.

The prescribed velocity profile for V_2 can be seen in Fig. 2. It is constructed such that the coresponding vorticity profile ξ_2 is proportional to $\sin(x)/x$ with $x = 2\pi r/a$ for $r < a$ and the vorticity vanishes for $r > a$. The total vorticity in this profile vanishes so that there are no winds for $r > a$. The magnitude of the wind profile is chosen such that the maximum wind is 40ms^{-1}. The external radius a is chosen to be 6000km. This profile and its parameters are representative of the stratospheric winter vortex variability and the vorticity profile resembles Fig. 2 of AH2002.

The layer thickness D_1, the thickness of the notional troposphere, is set at 8 km and the stratification parameter n_1, the density ratio between the notional stratosphere and troposphere, is set at 0.25. The gravitational acceleration g is set at its usual value. We can now solve Eq. 7 for any value of planetary vorticity f. All calculations have been repeated for a cyclonic vortex and an anticyclonic vortex. It is interesting to note that the calculations for the tropospheric winds, layer 1 in our model, is independent of the fact that there is a third layer overlying the stratosphere. In fact, we can equally think of our model atmosphere to be only composed of layers 1 and 2. The equation for the third layer velocity is the same as that of the first layer velocity apart from the stratification factor in front of the source term. This is the discrete layer version of the different penetration depth above and below the potential vorticity anomaly as discussed in detail in Scott and Dritschel (2005b).

3. Results

Equation 7 was solved using a relaxation scheme. The results are summarized in Fig. 3.

Figure 3a shows the ratio of the pressure changes at the pole between the troposphere and the stratosphere. The cusp in the anticyclonic curve is due to the transition from a geostrophically dominated regime at larger f to a cyclostrophically dominated regime at lower f. In the cyclostrophic regime all vortices are associated with a low central pressure. In the transition towards the geostrophic regime the polar pressure drop in the stratosphere exactly vanishes. For large planetary rotation the pressure change in the stratosphere is completely communicated to the troposphere. As can be seen in Fig. 3e the interface height perturbations at these rotation rates vanish so the change in atmospheric column weight in the troposphere at the pole is completely determined by the pressure change in the stratosphere.

Figure 3b shows the actual absolute value of the polar pressure change in the troposphere. At high rotation rates the pressure change is proportional to the planetary rotation, as is expected from geostrophic equilibrium: the pressure force balances the Coriolis force in the prescribed vortex in the stratosphere, and for high rotation rates this pressure gradient is exactly reproduced in the troposphere. For current planetary rotation rate (relative planet rotation of 1) the polar pressure change is about 10hPa, which is similar to the AH2002 result.

Figure 3c shows the ratio of the Rossby number between the troposphere and the stratosphere and Fig. 3d shows that actual Rossby number in the troposphere. The Rossby number is here defined as the maximum magnitude of the relative vorticity divided by the planetary vorticity f. For high rotation rates, the ratio of the Rossby numbers approaches n_1: because for these rotation rates the pressure change is the same in stratosphere and troposphere, the geopotential ratio, which is the same as the vorticity ratio, scales with the density ratio between stratosphere and troposphere. The actual tropospheric Rossby number has a maximum around current planet rotation rates. For very high rotation rates the pressure change in the troposphere is capped by the pressure change in the stratosphere so the Rossby number in the troposphere will scale with $1/f$. The behaviour for smaller rotation rates is quite complex with smaller Rossby number for smaller rotation rates because the tropospheric vortex becomes weaker but increasing Rossby number for the very smallest rotation rates because of the inverse proportionality with f.

Figure 3e shows the change in interface height between layers 1 and 2, the notional tropopause, at the pole. The values for current planetary rotation rate are remarkably realistic at about 300m and are the same as the AH2002 result. For very high rotation rates the interface becomes less and less flexible, as in Eq. 6. For low rotation rates the cyclostrophic balance for both the cyclonic and anticyclonic vortices prescribe a fixed geopotential structure, independent of f, with a raised tropopause over the pole. However, due to the smallness of f this raised tropopause only induces a small relative vorticity, proportional to f, through stretching of the troposphere.

Figure 3f shows the stratospheric Burger number as defined by the vorticity change, scaled by f, divided by the depth change, scaled by D_2, here set to 8km. This number measures the ratio of the vorticity contribution over the stratification contribution to the potential vorticity in the stratosphere. At current planetary rotation the Burger number is close to 1 which is realistic in the atmosphere and which was also assumed in the scaling arguments of AH2002. At higher rotation rates the potential vorticity field is most easily realized by a slight stretching of the column, corresponding to low Burger numbers, while the opposite is true for low rotation rates.

Figure 4 shows the profiles of the stratospheric and tropospheric relative vorticity for a cyclonic vortex at current planetary rotation. The tropospheric relative vorticity is proportional to the tropopause height and it compares well with Fig 3c of AH2002. Note that the tropospheric vorticity profile is broader than that of the inducing stratospheric vorticity with exponential tails beyond $r > a$.

4. Discussion and conclusions

A semi-analytical model for a vortex in gradient wind balance has been used to explore the direct interaction between the stratosphere and troposphere for varying planetary rotation. The aim was to clarify the apparent contradiction, as explained in the first section, between the the "light stratosphere" argument and the potential vorticity inversion argument.

The strength of the coupling between the stratospheric and tropospheric layers in our model depends in a fairly complex way on the planetary rotation rate. Furthermore, this coupling dependency is very different for different measures of coupling.

Perhaps the most simple and straightforward measure is the pressure change at the pole in the troposphere (Fig. 3b). This measure would be the one that is typically measured by pattern indices such as the North Atlantic Oscillation or Annular modes. This measure turns out to be highly dependent on the planetary rotation with a response largely much proportional to f in all regimes. Typically used covariance measures between stratospheric and tropospheric pressure patterns are similar to the measure in Fig. 3a with a nearly perfect coupling at high rotation rates and weak coupling at low rotation rates.

However, other measures such as given by the Rossby number give a different point of view. For the specific prescribed vortex structure the tropospheric Rossby number is strongest at current planetary rotation rates, probably because there the Burger number of the chosen vortex is close to one. However, compared to other measures, the tropospheric Rossby number remains relatively constant for the rotation rates examined.

These experiments point to weakness in the “light stratosphere” argument. It is clear that rotation and geostrophic balance is dominant at current rotation rates in determining the direct stratospere–troposphere coupling. But even at low rotation rates, outside the geostrophic regime, the resulting cyclostrophic balance determines the coupling between the stratosphere and troposphere. Perhaps counterintuitively, in this regime the coupling also depends strongly on f with a somewhat crude scale analysis showing that the vorticity perturbation in the troposphere is proportional to f while the tropospheric pressure perturbation is proportional to f^2. This means that for vanishing planetary rotation there is no coupling at all. In a steady state the gradient wind balance condition always plays a role and we cannot refer to the stratospheric influence on the troposphere without referring to the full balanced structure of the vortex.

Acknowledgments: The author received support of the AGU to present this work at the Chapman conference on Jets and Annular Modes.

References

Ambaum, M. H. P., and B.J. Hoskins, 2002: The NAO tropospherestratosphere connection. *J. Clim.*, **15**, 1969-1978.

Black, R. X., 2002: Stratospheric forcing of surface climate in the Arctic Oscillation. *J. Clim.*, **15**, 268-277.

Charney, J., and M.E. Stern, 1962: On the stability of internal baroclinic jets in a rotating atmosphere. *J. Atmos. Sci.*, **19**, 159-172.

Hartley, D. E., J.T. Villarin, R.X. Black, and C.A. Davis, 1998: A new perspective on the dynamical link between the stratosphere and troposphere. *Nature*, **391**, 471-474.

Haynes, P. H., and M.E. McIntyre, 1987: On the evolution of vorticity and potential vorticity in the presence of diabatic heating and friction or other forces. *J. Atmos. Sci.*, **44**, 828-841.

Hoskins, B. J., M.E. McIntyre, and A.W. Robertson, 1985: On the use and significance of isentropic potential vorticity maps. *Quart. J. R. Met. Soc.*, **111**, 877-946.

Kleinschmidt, E., 1950:, Über Aufbau und Entstehung von Zyklonen. I. Teil. *Meteor. Rundschau*, **3**, 1-7.

Scott, R. K., and D. G. Dritschel. 2005a: Downward Wave Propagation on the Polar Vortex. *J. Atmos. Sci.*, **62**, 3382-3395.

Scott, R. K., and D. G. Dritschel. 2005b: Quasi-geostrophic vortices in compressible atmospheres. *J. Fluid Mech.*, **530**, 305-325.

Figure captions

FIG. 1. Schematic of 3-layer atmosphere.

FIG. 2. Prescribed stratospheric velocity profile (solid) and corresponding relative vorticity profile (dashed). Both profiles are normalized with respect to their maximum values and the radial coordinate is rescaled with the external radius a.

FIG. 3. Balanced flow parameters as a function of planetary vorticity f scaled with the Earth's polar planetary vorticity of $1.4 \times 10^{-4}\mathrm{s}^{-1}$. See text for further details and discussion.

FIG. 4. Tropospheric (solid) and stratospheric (dashed) relative vorticity profile corresponding to current planetary rotation. Both profiles are normalized with respect to their maximum values and the radial coordinate is rescaled with the external radius a.

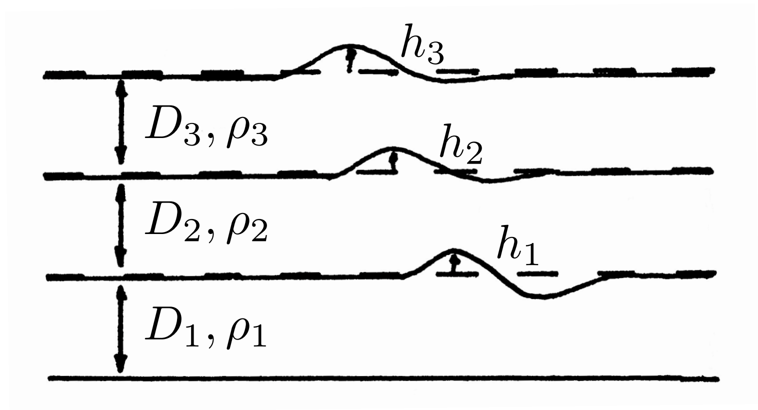

FIG. 1. Schematic of 3-layer atmosphere.

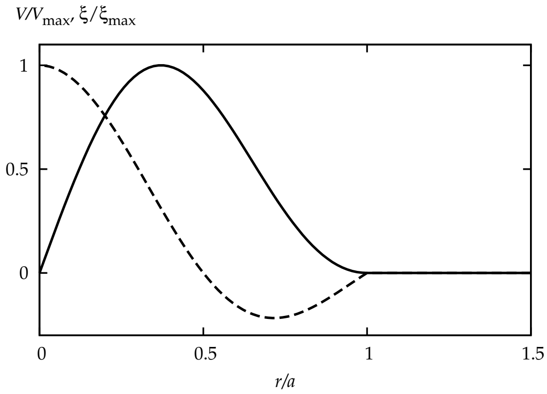

FIG. 2. Prescribed stratospheric velocity profile (solid) and corresponding relative vorticity profile (dashed). Both profiles are normalized with respect to their maximum values and the radial coordinate is rescaled with the external radius a.

$\sim$ Figure 2 $\sim$

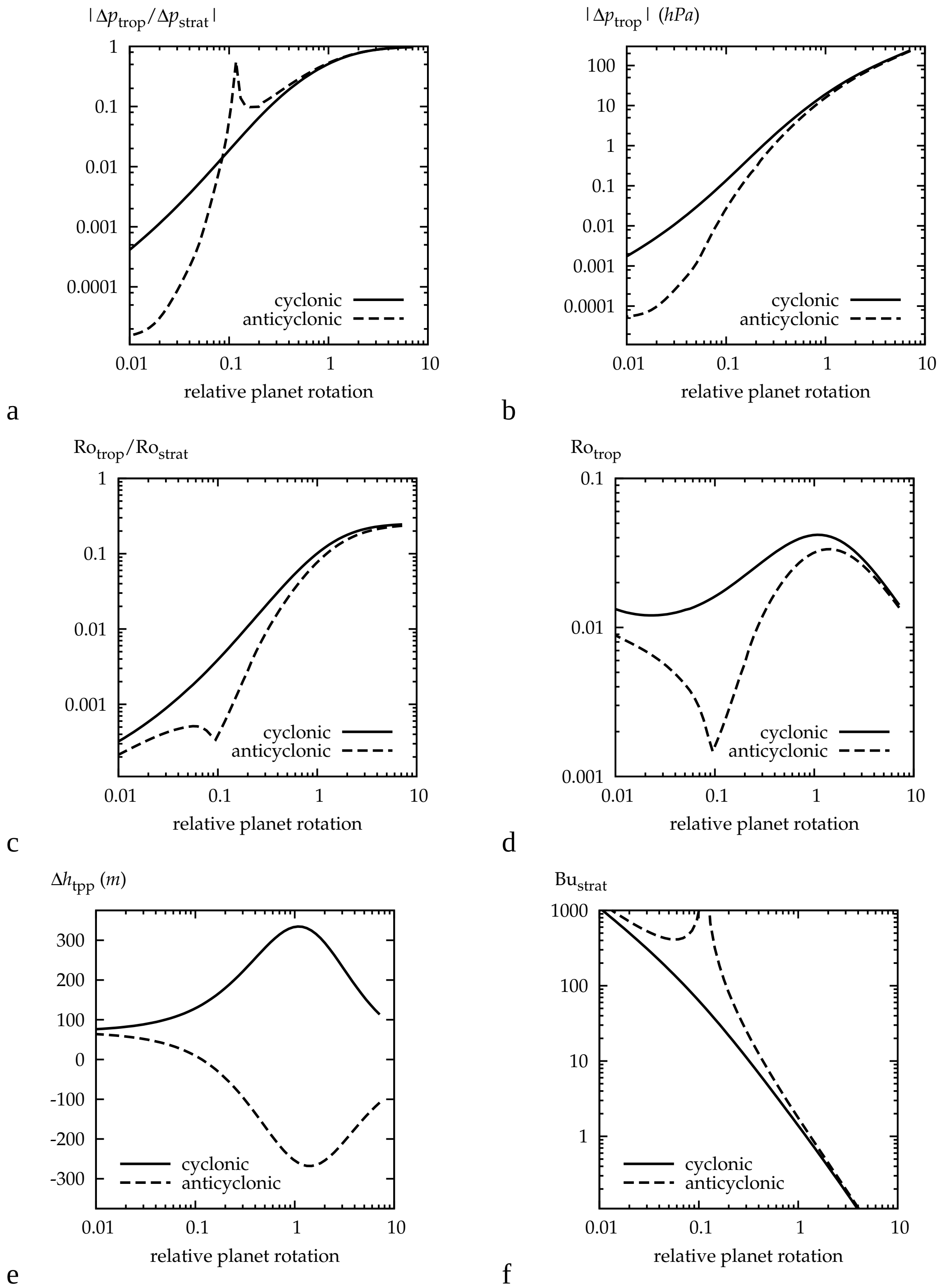

FIG. 3. Balanced flow parameters as a function of planetary vorticity f scaled with the Earth's polar planetary vorticity of $1.4 \times 10^{-4}\mathrm{s}^{-1}$. See text for further details and discussion.

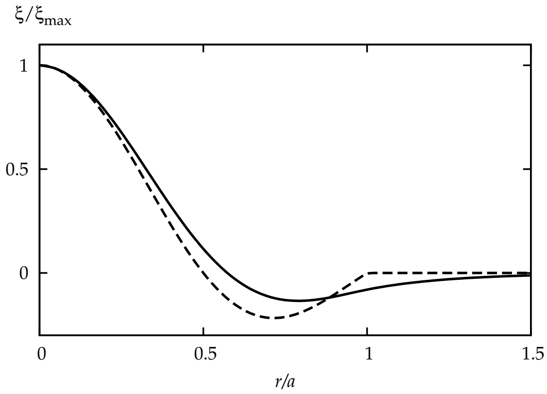

FIG. 4. Tropospheric (solid) and stratospheric (dashed) relative vorticity profile corresponding to current planetary rotation. Both profiles are normalized with respect to their maximum values and the radial coordinate is rescaled with the external radius a.